Contents

Chapter 1

Results and Analysis

In this chapter, the performance of the trained models is shown through various tables, plots, and visualizations. The focus is on showing the results of the final MLP regressor model, which performed best across all criteria. The following sections will provide detailed insights into the different analyses conducted to evaluate the model's effectiveness in assessing image quality in teledermatology.

1.1 Range of Distortion Values

The ranges of values for each distortion type were carefully chosen to reflect realistic scenarios for teledermatology applications. Each distortion type was visualized individually to make sure they were appropriate. **??** includes images that show each criterion with different distortion types and five severity levels.

It is important to note that images should not be normalized before viewing because normalization can make the images appear overly colorful and unrealistic. However, normalization is necessary during training and testing because the feature extraction backbone from ARNIQA was trained on ResNet50 with ImageNet images. This step helps the model accurately extract relevant features from the images.

1.2 Model Performance

1.2.1 Cross-Dataset Evaluation

The performance of the four different models was evaluated through cross-dataset testing. This involved assessing the models on both the SCIN and Fitzpatrick (F17K) datasets after synthetic distortion, as summarized in Table 1.1. This table highlights how well the models generalize across different datasets.

1.2.2 Parallel Coordinate Plot

The parallel coordinate plot in Figure 1.2 compares the best-performing models across seven criteria, including the overall SRCC. This visualization highlights the performance of the MLP Regressor, showing that it consistently outperforms the other models.

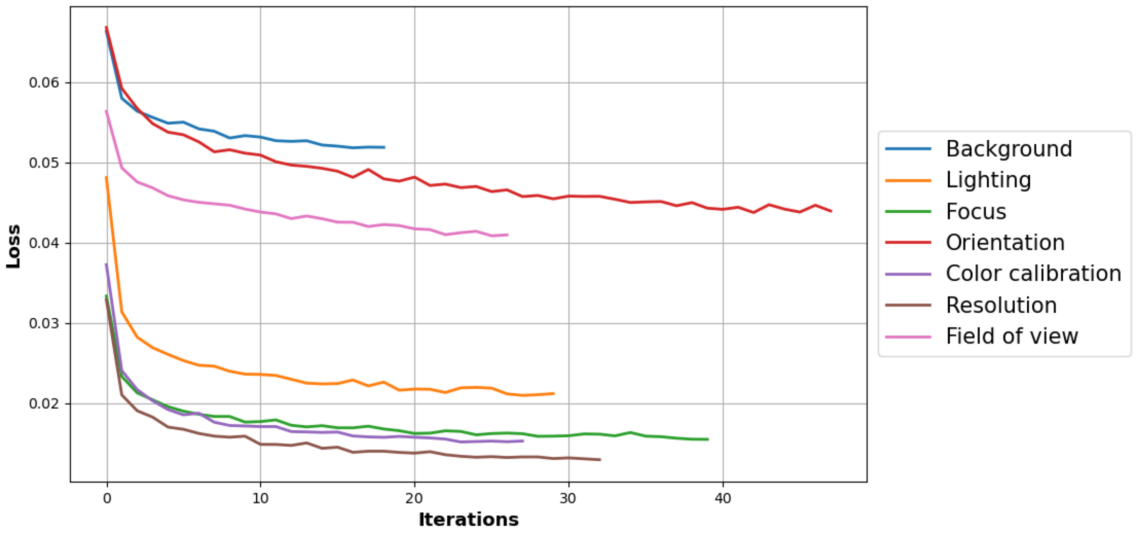

Figure 1.1: Loss curve showing the reduction in loss for each distortion criterion during the training process. Each line represents a different criterion, showing how the model's performance improves over time with each iteration. The maximum number of iterations was set to 500, and early stopping was enabled to prevent overfitting.

1.2.3 Performance Metrics

The performance of the final MLP regressor model on individual criteria is shown in Table 1.2. This table presents the performance metrics for the final MLP regressor model on 475 good quality Fitzpatrick images that were synthetically distorted. These metrics give a detailed view of the model's strengths and weaknesses.

Table 1.1: Spearman's Rank Correlation Coefficient (SRCC) of Different Models on SCIN and F17K Datasets. F17K refers to the Fitzpatrick17k dataset.

Model	**SCIN**	**F17K**
Combined MLP Regressor	<u>0.66</u>	<u>0.75</u>
Combined XGB Regressor	0.65	0.73
Combined XGB Classifier	0.58	0.61
Combined MLP Classifier	0.43	0.46
F17K MLP Regressor	0.54	0.69
SCIN MLP Regressor	0.62	0.49
F17K XGB Regressor	0.53	0.67
SCIN XGB Regressor	0.61	0.48
SCIN MLP Classifier	0.53	0.45
F17K MLP Classifier	0.47	0.58
SCIN XGB Classifier	0.54	0.43
F17K XGB Classifier	0.46	0.59

Table 1.2: Performance Metrics for Each Distortion Criteria

Criteria	**MAE**	**R^2**	**SRCC**	**Cohen's Kappa**
Background	0.9684	0.2595	0.5422	0.4399
Lighting	0.5726	0.6440	0.8028	0.7913
Focus	0.4042	0.7385	0.8622	0.8568
Orientation	0.9895	0.1824	0.4735	0.4102
Color calibration	0.4905	0.7334	0.8622	0.8583
Resolution	0.3642	0.7656	0.8722	0.8726
Field of view	0.5474	0.5976	0.7710	0.7660
Overall	**0.6195**	**0.5646**	**0.7507**	**0.7396**

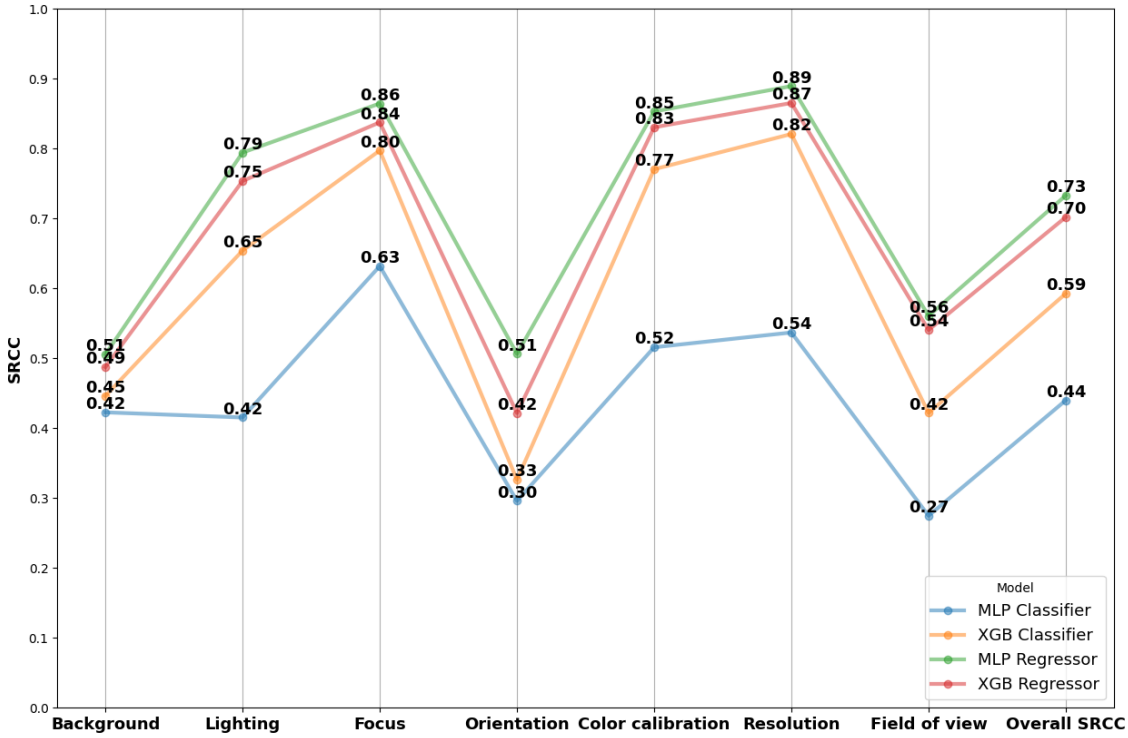

Figure 1.2: Parallel coordinate plot showing the best SRCC values for the four different models across the seven criteria and the overall SRCC. This plot highlights the performance of the MLP Regressor.

1.2.4 Confusion Matrices

In addition to numerical metrics, confusion matrices[1] were created for each criterion, as shown in Figure 1.3. These matrices display where the model makes correct predictions and where it makes mistakes, showing a detailed view of its accuracy for each type of distortion. Furthermore, the confusion matrices also reveal any biases the model might have toward certain severity ranges, indicating whether it tends to predict only low or high severity levels, or if its predictions are skewed in some way.

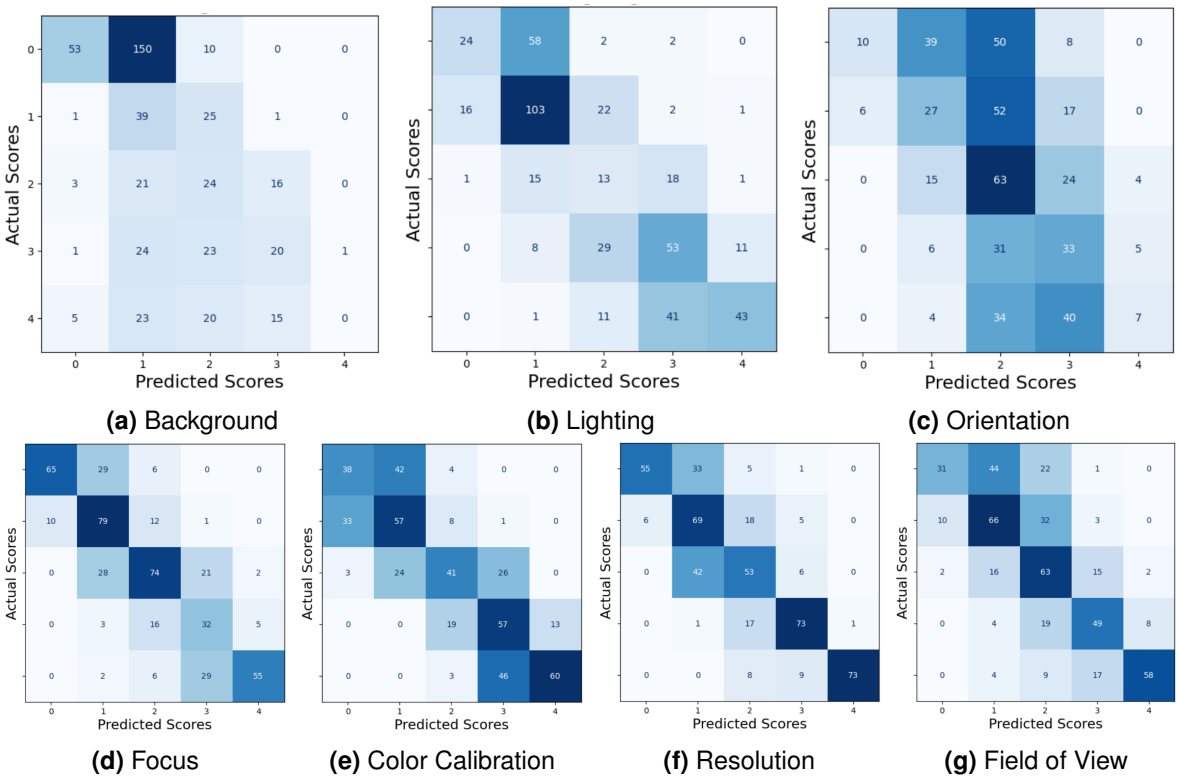

(a) Background **(b)** Lighting **(c)** Orientation

(d) Focus **(e)** Color Calibration **(f)** Resolution **(g)** Field of View

Figure 1.3: Confusion matrices for the MLP Regressor model evaluated on the 475 images from the Fitzpatrick dataset. Each matrix corresponds to a specific distortion criterion and shows the actual scores on the y-axis and the predicted scores on the x-axis. Darker shades indicate higher counts, highlighting where the model's predictions match the actual values and where discrepancies occur.

[1] from utils.visualization import plot_all_confusion_matrices

1.3 Model Predictions

To better understand the model's performance on the two test sets (70 synthetic distorted images and 200 authentic images), radar charts[2] were created. These charts show the criteria on the outside, with severity ranges going from the center (0) to the outer edge (1), indicating higher distortion for each criterion. These visualizations provide a clear and simple view of the model's performance, showing its strengths and areas for improvement.

1.3.1 Visualizations for Synthetic Distorted Images

These visualizations, as shown in Figure 1.4, help to compare the model's predictions with actual distortions for synthetic test images. This also helps to demonstrate the model's accuracy in predicting various types of distortions.

The first column shows the original image, the second shows the distorted image, the third contains the actual labels, and the fourth presents the model's predictions.

1.3.2 Visualizations for Authentic Images

The visualizations, as shown in Figure 1.5, compare the model's predictions with human-labeled scores for authentic images. This highlights the model's performance in real-world scenarios.

The first column shows the image, the second column displays the human-labeled scores, and the third column presents the model's predictions. This comparison helps show how well the model's predictions align with the human evaluations.

[2] from utils.visualization import plot_results

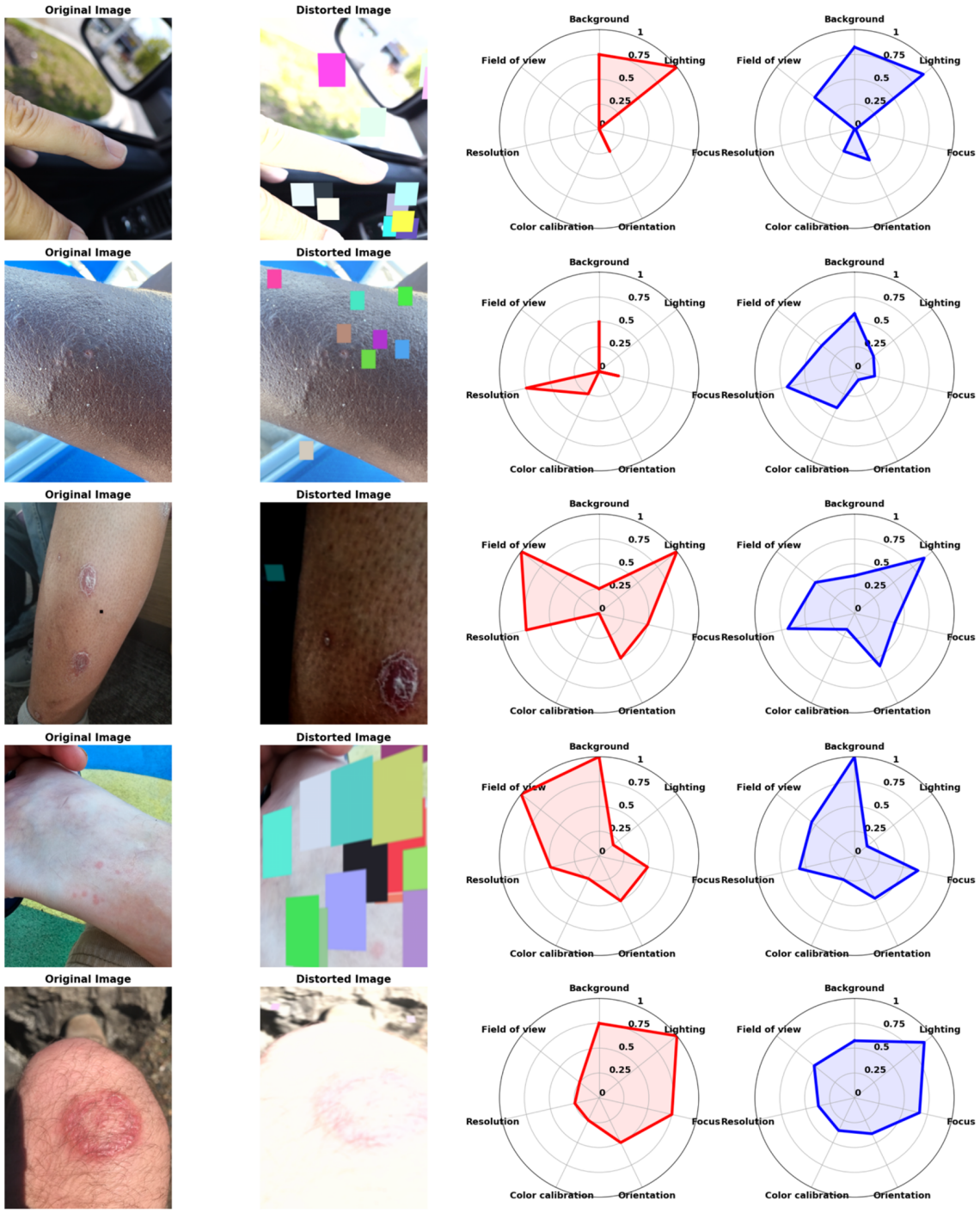

Figure 1.4: Visualizations for the MLP Regressor model on 70 synthetic distorted images. The four-column layout shows the original image, the distorted image, the actual labels, and the model's predictions.

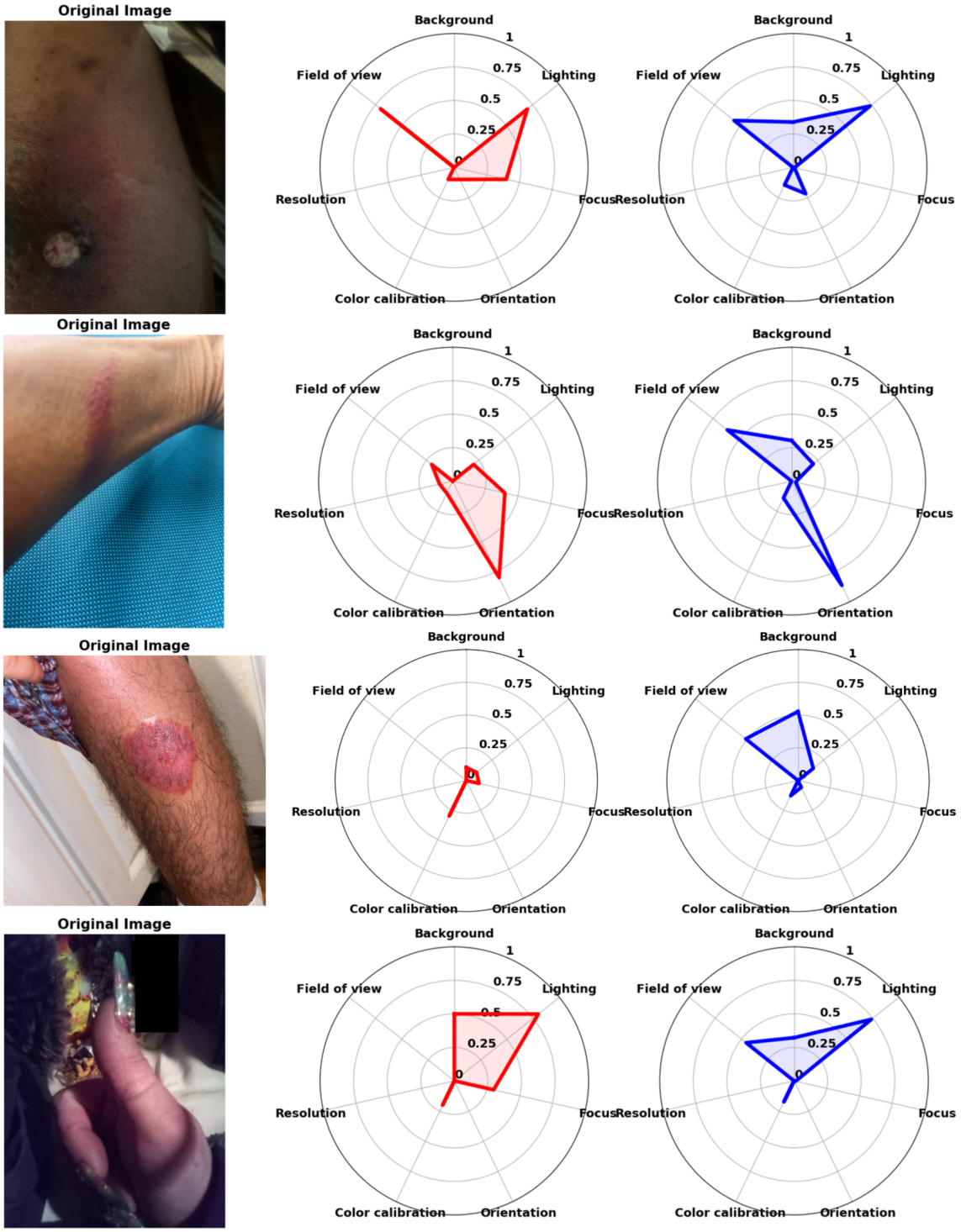

Figure 1.5: Visualizations for the MLP Regressor model on 200 authentic images. The three-column layout shows the image, the human-labeled scores, and the model's predictions.

1.4 Assessing Training and Testing Images Quality

To verify the quality of the images used for training and see how they change after synthetic distortion, radar charts were created. These charts show the quality of the original training images and how they are affected by the distortions. Additionally, the quality of both the synthetic and authentic test images is assessed using the same method. These radar charts show a simple visual representation of the quality and the level of distortion across the seven criteria.

1.4.1 Training Images Quality

Figure 1.6 and Figure 1.7 show the quality of the original SCIN and Fitzpatrick images, and the filtered good quality images, respectively. Figure 1.8 shows the quality of the combined SCIN and Fitzpatrick images and the synthetically distorted images used for training the model.

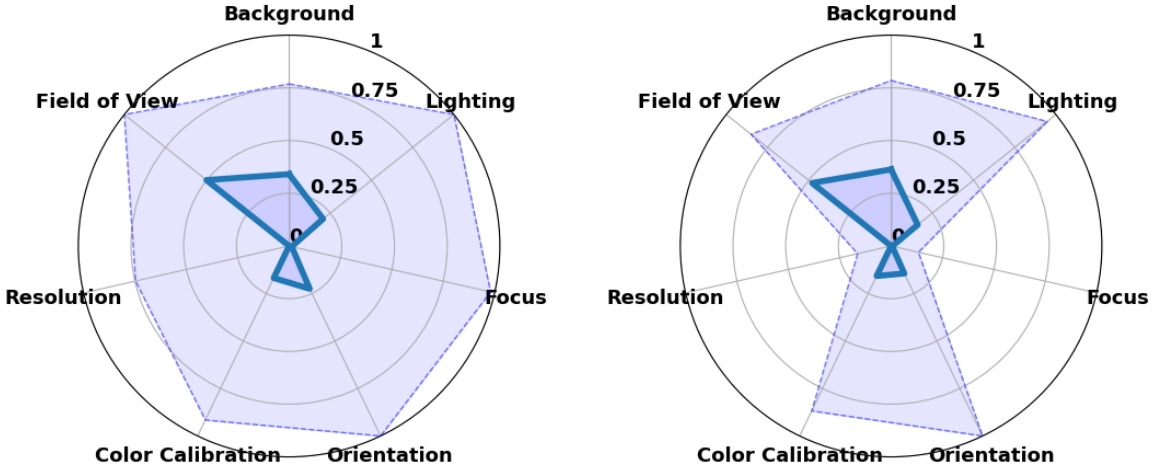

(a) SCIN Images

(b) Filtered SCIN Images

Figure 1.6: Radar charts for the SCIN dataset. (a) Original images from the SCIN dataset (10'379 images). (b) Filtered good quality images (475 images).

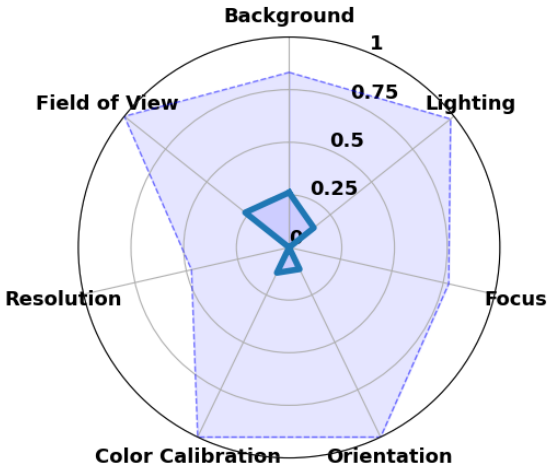

(a) Fitzpatrick Images

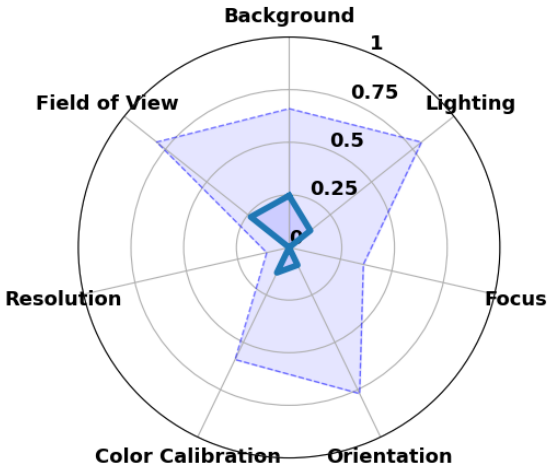

(b) Filtered Fitzpatrick Images

Figure 1.7: Radar charts for the Fitzpatrick dataset. (a) Original images from the Fitzpatrick dataset (16'577 images). (b) Filtered good quality images (475 images).

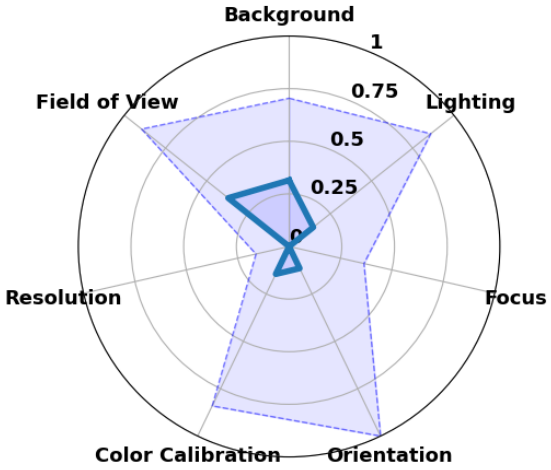

(a) Combined SCIN and Fitzpatrick Images

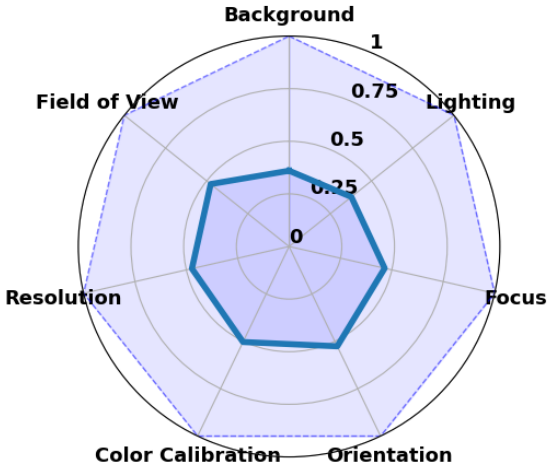

(b) Synthetically Distorted Images

Figure 1.8: Combined dataset analysis. (a) Combined SCIN and Fitzpatrick images (950 images). (b) Synthetically distorted images.

1.4.2 Test Images Quality

Figure 1.9 shows the quality of the filtered good quality test images and the synthetically distorted test images. Figure 1.10 shows the quality of the authentic test images from the SCIN dataset. These radar charts provide a visual representation of the quality of the test images and the level of distortion across the seven criteria.

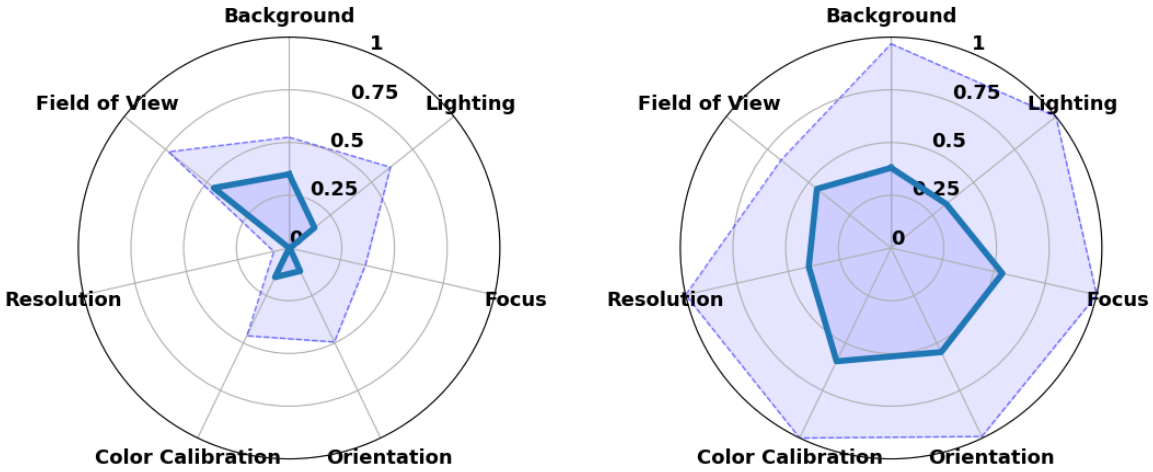

(a) Filtered Test Images

(b) Synthetically Distorted Test Images

Figure 1.9: Synthetic test set analysis. (a) Filtered good quality test images (70 images, independent of training set). (b) Synthetically distorted test images.

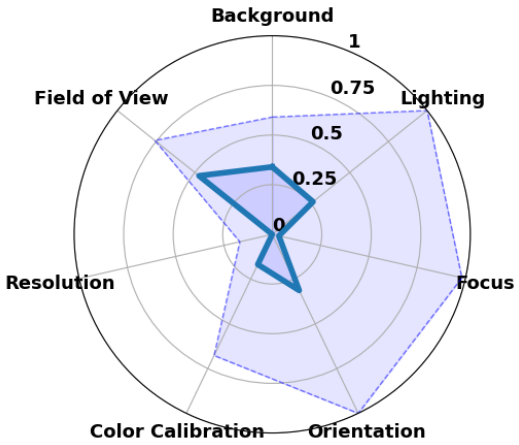

Figure 1.10: Authentic test set from the SCIN dataset, independent of the training images, showing real-world distortions.

1.5 Comparison with ARNIQA Predictions

This section compares the model's predictions with the predictions from ARNIQA for both synthetic and authentic test sets, highlighting how well the model aligns with established quality scores.

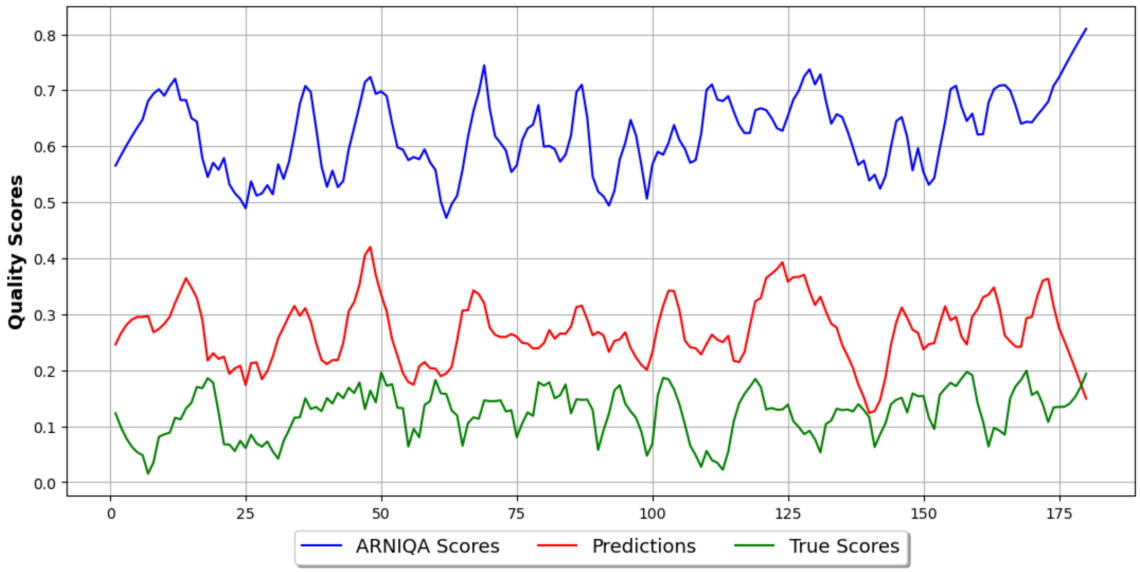

Figure 1.11: Comparison of ARNIQA Scores, Model Predictions, and True Scores for 200 authentic images from the SCIN Dataset. This plot presents the quality scores for each image, showcasing how well the model's predictions align with the ARNIQA scores and the true scores.

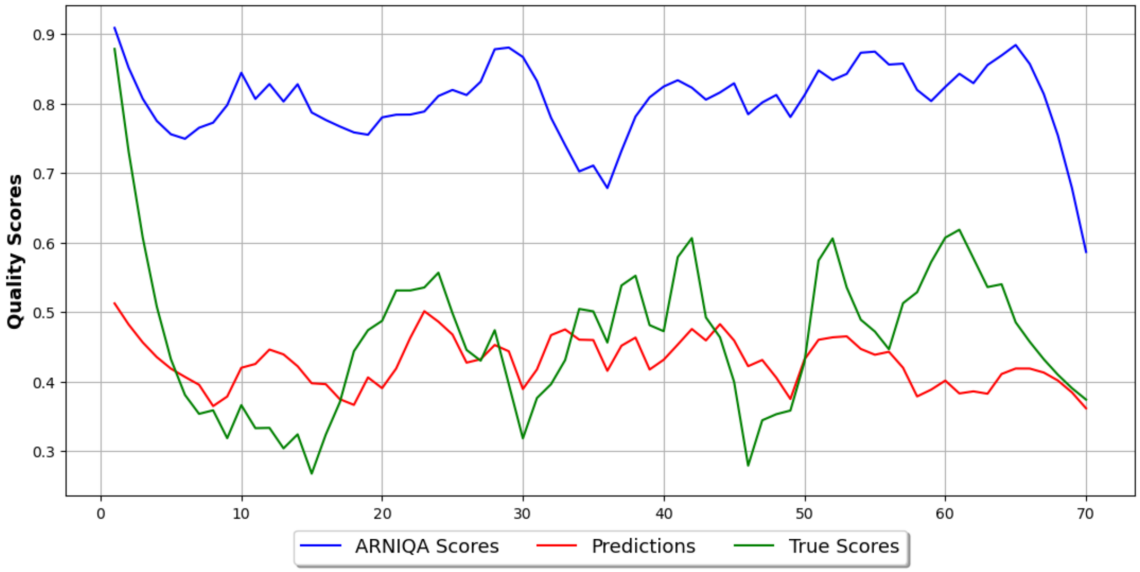

Figure 1.12: Comparison of ARNIQA Scores, Model Predictions, and True Scores for 70 synthetically distorted images from the SCIN dataset. This plot shows the quality scores for each image, highlighting the performance of the model against ARNIQA's predictions and the actual scores.

Chapter 2

Discussion

The chapter on Discussion covers the entire work and, in particular, the results achieved in Chapter 1. In the following sections, the results will be interpreted, the objectives of the thesis will be reviewed, and recommendations for future research in teledermatology image quality assessment will be provided.

2.1 Interpretation of Results

The differences in model performance shown in Figure 1.2 reveal that both classifiers (XGB Classifier and MLP Classifier) were not as effective as the regressors (XGB Regressor and MLP Regressor). This is likely because the task involves predicting continuous severity scores, which are more suited to regression models. Classifiers categorize the severity into fixed levels, which can lead to less precise predictions.

check this paragraph

The experiments demonstrated that the cross-dataset evaluation showed good generalization. The models performed well not only on the datasets they were trained on but also on previously unseen datasets. This indicates that the models, especially the MLP Regressor, can generalize well to different data distributions and are robust.

When we analyze the metrics in Table 1.2 alongside the confusion plots in Figure 1.3, it becomes clear that the criteria for focus, color calibration, and resolution are captured very well by the model. Although there are some fluctuations between the predicted severity and the actual severity, these deviations are typically only by one severity level. This minor difference suggests that the model is making reasonably accurate predictions. This high level of accuracy can be explained by the design of the ARNIQA backbone. When training ARNIQA to extract features, their goal was to assess general image quality, and they focused also on distortions related to focus and color calibration. Since I am using their backbone to extract features, the model performs better in these criteria.

On the other hand, lighting was also one of the distortions that ARNIQA focused on, but this criterion performed only moderately well. This can be reasonably explained by the fact that the lighting criterion includes two opposite types of distortions: brightening and darkening. If the majority of the training images were brightened and the validation set included darkened images, this could negatively impact performance. The model may struggle to accurately predict the lighting severity due to these opposing distortion types.

For the background criterion, it is clear from the confusion plot that there are rarely predictions on the higher severity levels. This is because, in the distortion pipeline, if the background proportion is less than 10% relative to the skin, no color blocks are added, resulting in a 0 value for background distortion. This indicates that many images were given a 0 value for background distortion. Additionally, when looking at the radar chart of the combined synthetically distorted images in Figure 1.8b, the median value for background distortion is lower than that of other criteria, indicating fewer strong severity values. This hypothesis that including more images with significant background presence can improve the model's performance is supported when examining the radar charts of filtered SCIN and filtered Fitzpatrick images in Figure 1.6 and Figure 1.7. The median severity for SCIN images is lower compared to the Fitzpatrick dataset. Moreover, the predictions for individual datasets also show differences. For example, **??** compares the metrics for background distortion between SCIN and Fitzpatrick using an MLP regressor. This table shows that the regressor trained on synthetically distorted SCIN images performs better on background. This further indicates that enhancing the training dataset with more background inclusive images could address this issue effectively.

The confusion plot also shows that the orientation criterion is generally uncertain in its predictions, tending to cluster around the middle severity levels. This might be due to the various perspective changes (top, bottom, right, left) applied during training. As a result, the model detects that there is some perspective distortion but cannot precisely determine the direction or severity, leading to predictions that hover around the middle severity levels.

For the last distortion, the field of view distortion, this criterion was the most experimental because this type of distortion is not as applicable to the general image domain. For teledermatology, it is crucial to have the lesion or area of interest centered in the image. However, in general photography, different rules like the golden ratio apply, where the subject is often placed off-center to create a more aesthetically pleasing composition. And, since ARNIQA is trained for general image quality assessment, it might have difficulties extracting features for field of view distortions specific to teledermatology.

I applied field of view distortions by cropping the upper left corner of the image in different scales, shifting the centered lesion to the bottom right corner. This method can introduce problems, such as having too much background in the upper left corner or not showing the lesion or skin at all in the image. This hypothesis can be validated by comparing the metrics between SCIN and Fitzpatrick images. The Table 2.1 show that Fitzpatrick images perform better in field of view distortion than SCIN images. This can be explained by the fact that SCIN images contain more background than Fitzpatrick images. Therefore, the field of view distortion criterion requires further refinement and targeted data collection to ensure the model can effectively handle these distortions.

Table 2.1: Performance metrics for field of view distortion using an MLP regressor on synthetically distorted SCIN and F17K images. F17K refers to the Fitzpatrick17k images.

Dataset	**MAE**	**R^2**	**SRCC**	**Cohen's Kappa**
SCIN (synthetically distorted)	1.20	0.05	0.23	0.08
F17K (synthetically distorted)	0.63	0.50	0.72	0.71

These observations highlight the strengths of using a combined dataset. By integrating diverse images from different sources, the model benefits from a wider variety of distortions and scenarios, enhancing its ability to generalize and perform well across different conditions.

2.2 Key Model Assumptions and Their Implications

The models assume that the features extracted by ARNIQA's backbone are comprehensive enough to capture the key distortions in teledermatology images. This assumption holds true for lighting, focus, color calibration, and resolution, covering 4 out of the 7 criteria. The remaining criteria: background, orientation, and field of view need further experimentation and fine-tuning. While the current performance indicates some level of effectiveness, more targeted data collection and model adjustments are necessary to fully validate these assumptions.

If the assumption that ARNIQA's backbone can capture all key distortions is not entirely correct, it would mean that the model might not perform well in real-world scenarios where these distortions are prevalent. To ensure these assumptions are valid, additional experiments with varied datasets and real-world images should be conducted. By expanding the variety of images used in training, particularly those with significant background presence, the model can be better equipped to handle real-world distortions. This is crucial for improving the model's robustness and generalizability.

While the backbone has proven effective for certain distortions, the uncertainties with background and orientation distortions highlight the need for further refinement. Addressing these uncertainties through targeted data collection and further model tuning can enhance the overall performance and reliability of the image quality assessment in teledermatology. Overall, the ARNIQA backbone shows great potential for teledermatology applications, but continuous improvement and validation are essential to achieve the best possible performance.

2.3 Reviewing the Objectives of the Thesis

At the beginning of this thesis, the specific objectives were detailed:

- An extensive review of the literature on image quality assessment (IQA) methods, focusing on their application in teledermatology.
- Identifying and selecting image quality metrics that are most suitable for assessing the quality of dermatological images.
- Evaluate the performance of selected image quality metrics on dermatological datasets to determine their effectiveness in assessing image quality.
- Develop a reproducible repository of image quality assessment tools and methodologies for teledermatology applications.

The first objective involved carrying out an in-depth review of the literature on image quality assessment methods and their application in teledermatology. This took a lot of time but was very important for the rest of the work. Through this review, key concepts such as IQA, teledermatology, ARNIQA, and related works were explored and documented.

The second objective was achieved during the literature review process. In this phase, the seven quality criteria from ISIC were identified and chosen as the best metrics for assessing the quality of dermatological images. This selection was critical for the next steps.

For the third objective, the performance of the selected image quality metrics was evaluated on dermatological datasets. These evaluations were thorough, involving tests on independent images not included in the model training. The datasets included both synthetically distorted

images and images with authentic distortions, ensuring a complete assessment of how well the metrics worked.

The final objective was to develop a reproducible repository of image quality assessment tools and methods for teledermatology applications. This was successfully accomplished, making it possible for further experiments and research to build on this thesis. The repository provides a solid framework for future work in this field, ensuring that the methods and tools developed here can be effectively used and expanded upon.

2.4 Comparison with Related Work

2.5 Reflection

2.6 AI Tools Used

In this work, several AI tools were used. ChatGPT was used to compress and summarize content. Additionally, it was used to optimize sentences and sections to make them more reader-friendly. Furthermore, GitHub Copilot was used in the development environment. It primarily helped in developing the Python scripts and models. These tools made the work more efficient and helped improve the overall quality of the thesis.

Chapter 3

Conclusion and Future Work

text

Chapter 4

Chapter

Ausblick
Reflexion der eigenen Arbeit, ungelöste Probleme, weitere Ideen.

4.1 Section

text